



Validation of SWAY Wind Turbine Response in FAST, with a Focus on the Influence of Tower Wind Loads

Preprint

J. H. Koh

*School of Mechanical and Aerospace Engineering,
Nanyang Technological University*

A. Robertson, J. Jonkman, and R. Driscoll
National Renewable Energy Laboratory

E. Yin Kwee Ng

*School of Mechanical and Aerospace Engineering,
Nanyang Technological University*

*To be presented at the International Offshore and Polar
Engineering Conference (ISOPE 2015)*

Kona, Hawaii

June 21–26, 2015

**NREL is a national laboratory of the U.S. Department of Energy
Office of Energy Efficiency & Renewable Energy
Operated by the Alliance for Sustainable Energy, LLC**

This report is available at no cost from the National Renewable Energy Laboratory (NREL) at www.nrel.gov/publications.

Conference Paper

NREL/CP-5000-63569

April 2015

Contract No. DE-AC36-08GO28308

NOTICE

The submitted manuscript has been offered by an employee of the Alliance for Sustainable Energy, LLC (Alliance), a contractor of the US Government under Contract No. DE-AC36-08GO28308. Accordingly, the US Government and Alliance retain a nonexclusive royalty-free license to publish or reproduce the published form of this contribution, or allow others to do so, for US Government purposes.

This report was prepared as an account of work sponsored by an agency of the United States government. Neither the United States government nor any agency thereof, nor any of their employees, makes any warranty, express or implied, or assumes any legal liability or responsibility for the accuracy, completeness, or usefulness of any information, apparatus, product, or process disclosed, or represents that its use would not infringe privately owned rights. Reference herein to any specific commercial product, process, or service by trade name, trademark, manufacturer, or otherwise does not necessarily constitute or imply its endorsement, recommendation, or favoring by the United States government or any agency thereof. The views and opinions of authors expressed herein do not necessarily state or reflect those of the United States government or any agency thereof.

This report is available at no cost from the National Renewable Energy Laboratory (NREL) at www.nrel.gov/publications.

Available electronically at SciTech Connect <http://www.osti.gov/scitech>

Available for a processing fee to U.S. Department of Energy and its contractors, in paper, from:

U.S. Department of Energy
Office of Scientific and Technical Information
P.O. Box 62
Oak Ridge, TN 37831-0062
OSTI <http://www.osti.gov>
Phone: 865.576.8401
Fax: 865.576.5728
Email: reports@osti.gov

Available for sale to the public, in paper, from:

U.S. Department of Commerce
National Technical Information Service
5301 Shawnee Road
Alexandria, VA 22312
NTIS <http://www.ntis.gov>
Phone: 800.553.6847 or 703.605.6000
Fax: 703.605.6900
Email: orders@ntis.gov

Cover Photos by Dennis Schroeder: (left to right) NREL 26173, NREL 18302, NREL 19758, NREL 29642, NREL 19795.

NREL prints on paper that contains recycled content.

Validation of SWAY Wind Turbine Response in FAST, with a Focus on the Influence of Tower Wind Loads

Jian Hao Koh

School of Mechanical and Aerospace Engineering, Nanyang Technological University
Singapore

Amy N. Robertson

National Renewable Energy Laboratory
Golden, Colorado, United States of America

Jason M. Jonkman

National Renewable Energy Laboratory
Golden, Colorado, United States of America

Frederick Driscoll

National Renewable Energy Laboratory
Golden, Colorado, United States of America

Eddie Yin Kwee Ng

School of Mechanical and Aerospace Engineering, Nanyang Technological University
Singapore

ABSTRACT

Using data obtained from open-sea testing of the 1:6.5 scale prototype of the SWAY hybrid tension-leg spar-type floating wind turbine, a FAST model of the SWAY system was built and validated. Significant in the validation process were improvements to the FAST wind turbine simulation tool to incorporate wind loading on the turbine tower for floating systems. Simulations were performed with and without the new tower-load capability to examine its influence on the response characteristics of the system. This is important in situations when the turbine is parked in survival conditions. The simulation results were then compared to measured data from the SWAY system in both turbine operating and nonoperating conditions. Mixed results were observed when comparing the simulated system behavior to the measured data, but the tower wind loads improved the comparison for nonoperating conditions.

KEY WORDS: offshore wind turbine; floating; spar-type; FAST; simulation; open-sea testing; validation.

INTRODUCTION

Verification and validation of complex aero-hydro-servo-elastic wind turbine simulation tools are critical to ensuring their accuracy in predicting the response of floating offshore wind systems. FAST, developed by the National Renewable Energy Laboratory (NREL), is one of the numerical simulation tools available that can model floating wind turbines. FAST simulation results have been compared to measured data for a variety of floating offshore wind systems,

including both tank tests and open-ocean demonstration systems.

Using the data obtained from open-sea testing of the 1:6.5th-scale prototype of the SWAY hybrid tension-leg spar-type floating wind turbine, a FAST model of the SWAY system has been built and validated. This paper gives an overview of the SWAY prototype system, modeling work of the system performed in FAST, and testing that was performed with the demonstration system. The paper then focuses on the improvements made to the FAST tool to incorporate wind loading on a wind turbine tower for floating systems. The new features include an option to use a provided table of drag coefficients ($C_{D,tower}$) based on the Reynolds number for cylindrical towers, or to manually input the cross-section $C_{D,tower}$ values. Simulations with and without tower loads were carried out in nonoperating and operating conditions, and compared with experimental data for those conditions. Finally, limitations of the FAST model and potential areas of improvement are discussed.

MODELING OF SWAY WIND TURBINE

Modeling Tools

In this study, the offshore wind modeling tool, FAST version 7 (v7.02.00d-bjj), was used. Since this work began, a newer version of FAST was released (v8.09.00a-bjj), but it was not available in time for use in this project. FAST v7 employs a combined modal and multibody system (MBS) approach for modeling the structural dynamics of offshore wind systems. A separate finite element method pre-processor, BModes (v1.03.01) developed by Bir (2007), was used to compute the

coupled mode shapes for the wind turbine blades. Tower modes can also be derived using BModes, but for this work the tower was modeled as a rigid body. A detailed description of the theory, code and numerical solution techniques can be found in the FAST Theory Manual (J. Jonkman, 2014) and FAST User's Guide (J. Jonkman and Buhl, 2005), and at the National Wind Technology Center (NWTCC) website.

Hydrodynamic load and mooring system calculations were processed by the HydroDyn module coupled with FAST. Both regular and irregular waves can be introduced, with irregular waves defined using either a JONSWAP spectrum, Pierson-Moskowitz (PM) spectrum or a user-defined wave spectrum (used in this study). The module was developed by J. M. Jonkman (2009) and full details can be found in his dissertation (J. M. Jonkman, 2007).

To obtain the hydrodynamic parameters required by HydroDyn, radiation and diffraction problems were solved using the boundary integral equation method in the frequency domain based on the platform geometry using WAMIT (Wave Analysis at Massachusetts Institute of Technology) v6.416 (WAMIT, 2012).

To compute the blade aerodynamics in FAST, AeroDyn version 13 (v13.00.02a-bjj) was used. AeroDyn is a strip-theory-based horizontal axis wind turbine aerodynamics analysis code that has the option of using either blade element momentum (BEM) theory (used in this study) or generalized dynamic wake theory. This code also includes a model of unsteady airfoil aerodynamics, including dynamic stall. In this work, in which a downwind configuration is used, it is important to discuss the tower influence on blade aerodynamics. The tower shadow model used in AeroDyn is based on a potential flow solution developed by Bak, Madsen and Johansen (2001) and supplemented by a tower wake (velocity deficit) model from the work of Powles (1983). Further details are discussed in the AeroDyn User's Guide (Laino and Hansen, 2002), AeroDyn Theory Manual (Moriarty and Hansen, 2005) and Addendum to the User's Guide for FAST, A2AD, and AeroDyn (Jonkman and Jonkman, 2013).

AirfoilPrep (v2) is a spreadsheet developed by NREL for users to generate airfoil data files required by AeroDyn. In this study, it was used to generate 360-degree data of the airfoil data input files using the Viterna and Janetzke (1982) method. The spreadsheet was also used to interpolate the aerodynamic coefficients for other span locations and for applying three-dimensional delayed stall corrections caused by blade rotation using the method proposed by Du and Selig (1998), and Eggers and Digumarthi (1992).

To generate the simulated inflow turbulence environment for aerodynamic calculations, TurbSim (v1.06.00) was used to generate full-field flows. TurbSim can use various wind spectral models, coherence models, coherent turbulence structures, and wind profiles that are specified by the International Electrotechnical Commission (IEC) standards (used in this study), and non-IEC models. The details of the TurbSim code are found in the TurbSim User's Guide (B. J. Jonkman and Kilcher, 2012).

Modeling Summary and System Coordinates

The details of the SWAY turbine model, experimental testing and instrumentation have been introduced by Koh, Robertson, Jonkman, Driscoll, and Ng (2013) in a previous paper. Table 1 provides a summary of the SWAY prototype floating wind turbine properties, and Fig 1 is an illustration of the system. The SWAY prototype uses a spar-type support structure, a three-bladed downwind turbine, and a single tension-rod system for station-keeping and providing the static stability of the wind turbine in platform pitch. Universal joints attach the tension

rod to the bottom of the spar and to a large steel mass (gravity anchor) on the seafloor using universal joints. In addition to the single leg anchor system, the key components in the system are unique spreader beams and tension cables, which help to stiffen the tower and reduce fatigue loads, and allow the tower to carry a larger turbine.

The experimental data come from the test conducted between June 2012 and September 2013. In addition to the instrumentation described in earlier work of Koh et al. (2013), data were used in this paper from a tower wave height sensor that measures the wave height near the tower base using an ultrasonic transducer. As this measurement is influenced by the heave motion of the system, the final wave data were a result of adding the heave motion to the heave sensor data. The advantage of using the tower wave height signal rather than measurements from the Acoustic Wave and Current meter (AWAC) is the increased sampling rate of 100 Hz by the Bachmann controller, compared to the 1-hr average supplied by the AWAC.

Fig. 1 shows the coordinate system used for the results reported in this paper. The translational (surge, sway and heave) and rotational (roll, pitch and yaw) degrees of freedom (DOFs) of the platform are referenced from an origin located at the mean sea level (MSL) at the center of the tower when vertically upright.

Table 1. SWAY 1:6.5 scale wind turbine prototype specifications.

Support Structure Manufacturer	SWAY
Model of Turbine	SWAY 1:6.5 Scale Prototype
Production Year of Turbine	2011
Rated Power	7 kW
Rotation Axis	Horizontal
Orientation	Downwind
Number of Blades	3
Rotor Diameter	14.9 m (after extension in 2012)
Hub Height	13.133 m
Control	Individual Pitch Control
Tower Type	Tubular
Floater Type	Spar Buoy
Cut-In Wind Speed	2 m/s
Rated Wind Speed	6 m/s
Cut-Out Wind Speed	16 m/s

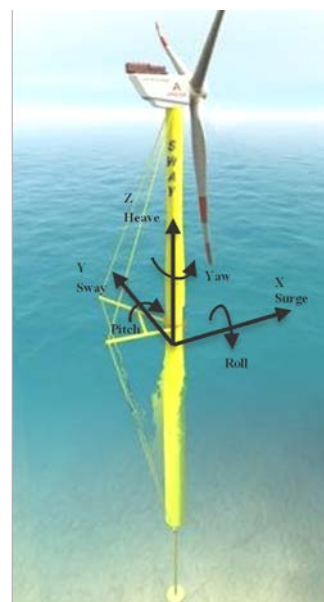


Fig. 1. SWAY turbine, coordinate systems and platform DOF (Koh et al., 2013).

CALCULATION OF TOWER LOADING

In the publicly released version of FAST v7 and AeroDyn v13, the drag forces from the wind on the tower and nacelle are not calculated. During the initial analysis of the simulation cases, the authors speculated the importance in including tower loading to the SWAY system in conditions in which the turbine blades are not rotating.

To account for the tower drag, changes were made to FAST to calculate the wind loading on each tower element at each simulation time-step. The approach used assumes that the tower is a cylinder, either tapered or un-tapered, and has limited application to multimember or lattice-type towers. Several strategies for accounting for wind loading on towers are available from both industrial standards and other researchers. For example, the International Standards Organization (ISO) 4354 (2009) standard describes the total wind load as a combination of three components. The first is the mean component caused by the mean wind speed. The second is the fluctuating (background) component, which results from the unstable nature of flow around bluff bodies including buffeting, flow separation, re-attachments, and vortex shedding. Other transient loads can also be induced by the motion of the structure caused by the wind such as galloping or flutter. The third is the “resonant” component, which results in a phenomenon called lock-in (Holmes, 2007) or vortex-induced vibration, which occurs when the frequency of vortex shedding is similar to the frequency motion of the body. For the majority of structures, the resonant component is small, and as suggested by Scruton (1981) and ISO 4354 (2009), the assumption of static loads as a result of wind is reasonably adequate unless the structure is large, lightweight, and lightly-damped. Although this assumption may not be fully applicable to a wind turbine tower, because of difficulties and uncertainties in quantifying the fluctuating component in a time-domain simulation, only the mean component of the wind force with effects of natural freestream turbulence is considered in this code improvement.

The code improvement is summarized in the simulation flowchart illustrated in Fig. 2. First, FAST checks the platform input file for the platform load model (PtfmModel) value set by the user. If the value (4) is set to include tower loading, FAST will read the tower drag coefficient and tower diameter values from the tower input file. Next, FAST checks the type of wind inflow data used. If TurbSim-generated wind inflow data are used, it obtains the lowest Z-position of the wind data defined as GridBase. As a result, the wind inflow for the region below GridBase is undefined as shown in Fig. 3. It is a common practice to only define wind inflow data for the expected region of turbine blade motion as generation of a larger area of wind inflow is limited by computational cost and limited memory.

Next, for every simulation time step and tower node, FAST checks the position of the tower node and retrieves the undisturbed wind velocity from the wind inflow data if the position is equal or more than the GridBase value. If the position is less than the GridBase value, the wind inflow data for the undefined region (which is needed for the tower drag calculations) are obtained by assuming that the wind profile from the GridBase to the MSL follows the power law (Eq.1). The exponent $\alpha = 0.140$ is recommended by the IEC 61400-3 (2009) for offshore wind conditions.

$$U_z = U_{GridBase} \left(\frac{z}{GridBase} \right)^{0.140} \quad (1)$$

With the wind inflow data obtained, the magnitude of the drag force per unit length is calculated using Eq. 2 and added vectorially along the relative wind direction to the overall platform and tower loads calculation for every time step.

$$D_{tower} = \frac{1}{2} \rho \left((V - V_{tower}) \right)^2 C_{D,tower} d_{tower} \quad (2)$$

D_{tower} is the drag force per unit length of the tower element, ρ is the density of air, $(V - V_{tower})$ is the magnitude of the difference between the undisturbed inflow velocity (with turbulence) and the velocity of the tower element at the tower element location (V_{tower}). $C_{D,tower}$ is the drag coefficient of the tower element, and d_{tower} is the diameter of the tower element.

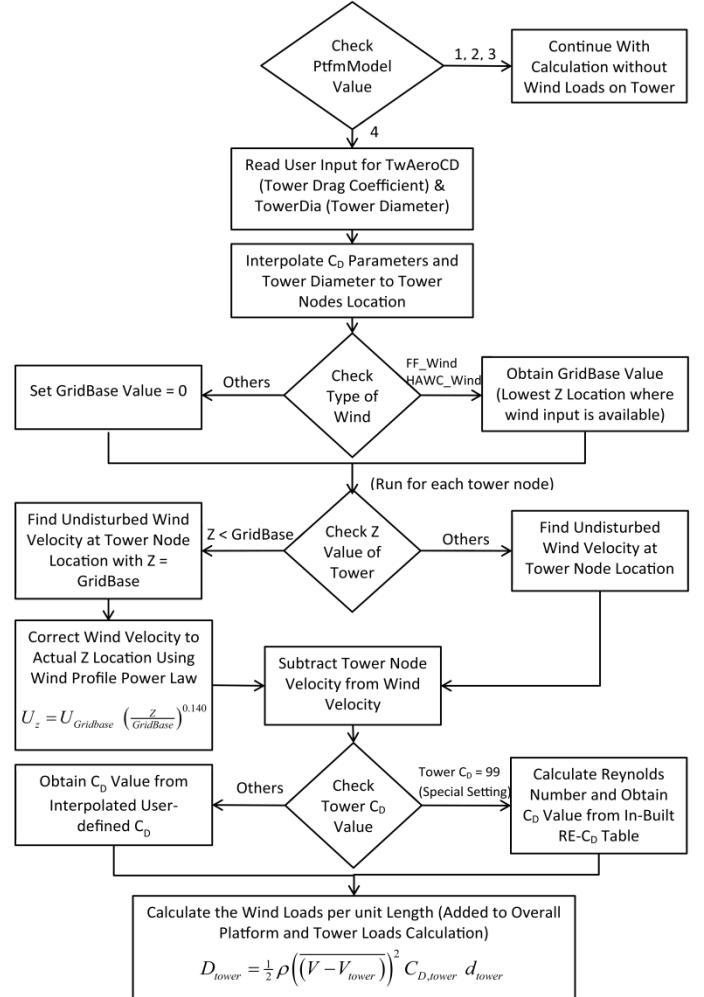


Fig. 2. Simulation flow chart for calculation of tower loading.

It is also commonly known that factors such as aspect ratio, surface roughness, turbulence intensity and the Reynolds number may affect the $C_{D,tower}$ for circular cylinders. For example, Roshko (1961) and Wieselsberger (1921) described the various flow regimes, the occurrence of the critical Reynolds number and drag coefficient values for a circular cylinder with a smooth surface across different Reynolds number. Scruton, Rogers, Menzies, and Scorer (1971) showed that a reduction in drag coefficient occurs for a circular cylinder of finite aspect ratio with a single free end. The surface roughness effect on lowering the critical Reynolds number range is also shown in E.S.D.U. 80025 (1986).

Because of the high variability and numerous factors, the drag coefficient of the tower was designed to be manually entered by the user. This gives the user a certain degree of control, which can be useful in accounting for wind loads for nontubular towers or utilizing a

drag coefficient prescribed specifically for individual tower designs or standards such as the ISO 4354 (2009) and EN 1991-1-4 (2005). Otherwise, the user can use the default $Re-C_{D,tower}$ table (plotted in Fig. 4 and used in this study), which is applicable for a circular smooth cylinder of high aspect ratio. The data are obtained from the work of Roshko (1961) and Wieselsberger (1921). The Reynolds number of the flow is calculated based on Eq. 3.

$$Re_{tower} = \frac{(V - V_{tower}) \times d_{tower}}{\nu} \quad (3)$$

where ν is the kinematic viscosity of air.

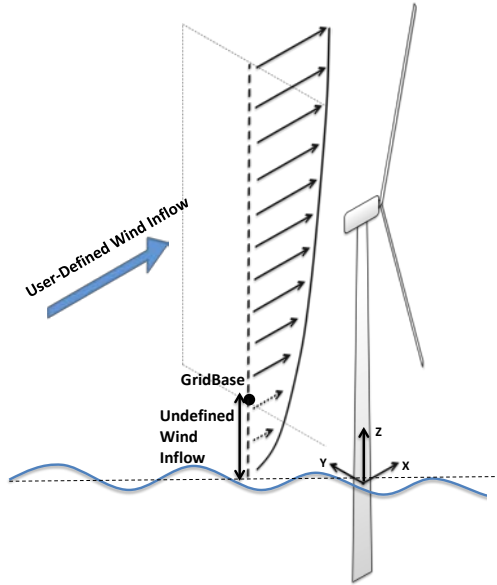


Fig. 3. Undisturbed wind inflow along the rotor and tower.

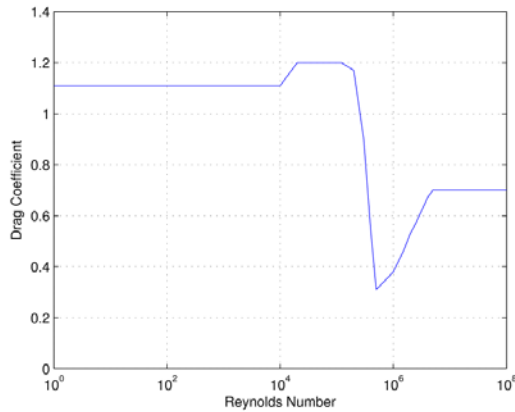


Fig. 4. $Re-C_{D,tower}$ graph.

MODEL VALIDATION

One nonoperational case and one operational case were selected for comparison to examine the influence of tower drag load and to validate against measured data from the SWAY prototype.

Selection of Test Cases

Nonoperating Case

From the large amount of data sets recorded, it is important to start the validation work with simple test cases that have stable conditions over an extended period of time. Therefore, one 10-min dataset (Non-Op

Case) was selected with the following criteria for the ease of modeling in FAST:

- 1) Instruments operating without abnormalities
- 2) Zero or very low rotor speed values
- 3) Mean wind speed of the preceding two 10-min test cases has less than 5% in variation from the selected test case
- 4) Mean wind direction of the preceding two 10-min test cases has less than 5° in variation from the selected test case

The criteria are focused on reducing any transient motion generated by the conditions before the actual test case. The one 10-min test case that was selected had a mean wind speed of 14 m/s with significant wave height of 0.65 m. This is one of the highest wind speed conditions that fulfilled the selection criteria. The wind, wave and current conditions are summarized in Fig. 5.

Operating Case

One 10-minute operational test case (Op Case) in control region III was selected for analysis and validation. The test case chosen was selected due to the stable wind velocity and rotor speed over an extended period of time. As the control algorithm from the real system was not available in the numerical model, this test case was also selected because of its limited variations in blade pitch angle to minimize the effects of the lack of control system. The test case had an average rotor speed of 33.67 rpm with a mean wind speed of 7.32 m/s measured at the anemometer height. The measured time series data of the rotor speed and blade pitch angle are shown in Fig. 6, whereas the wind, wave and current conditions are shown in Fig. 5.

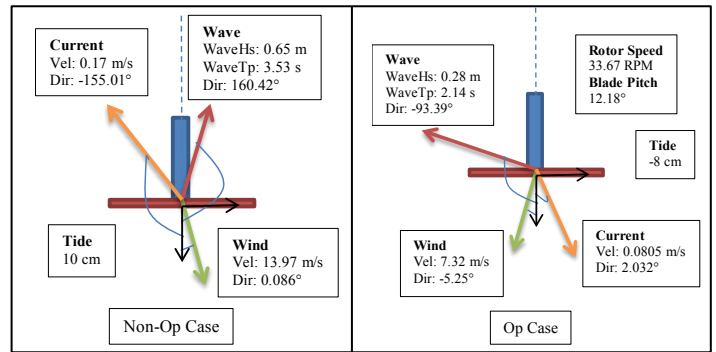


Fig. 5. Conditions for test cases.

Generating Wind Inflow Files

The wind inflow files used by AeroDyn were generated using TurbSim with the settings shown in Table 2. The mean wind speed and turbulence intensity were obtained from the sonic anemometer readings at the boom (Koh et al., 2013). Note that the minor yaw error (shown as wind direction in Fig. 5) is a result of the system being a free yaw system. This error was represented as a yaw offset in FAST. The analysis time was set at 1200 s, to allow for 10 minutes of data after any initial transient behavior had died out. The vertical and horizontal grid-point sizes were set such that they were approximately the mean chord length of the blade.

The turbulence model was assumed to follow the IEC Kaimal spectral normal turbulence model (B. J. Jonkman and Kilcher, 2012) and the turbulence intensity and reference wind speed were derived from sonic anemometer readings of wind speeds from the two different test cases. The power law exponent and surface roughness length are recommended values from the IEC 61400-3 (2009).

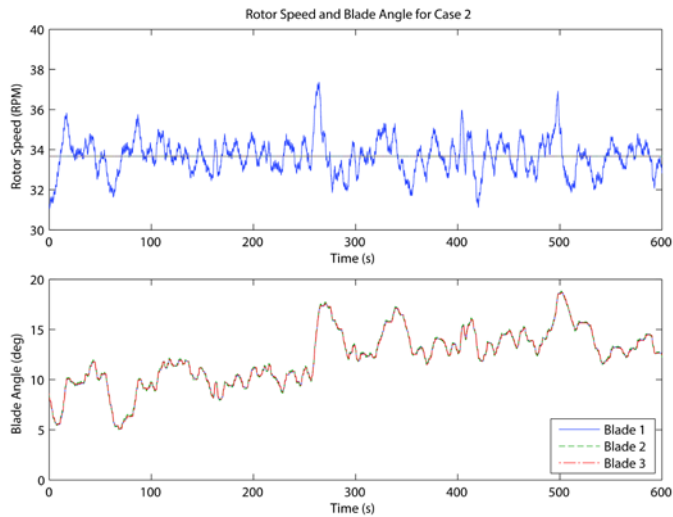


Fig. 6. Rotor speed and blade pitch angle for Op Case.

Table 2. TurbSim wind inflow properties for test cases.

	Non-Op Case	Op Case
Hub Height [m]	13.133	
Grid Height [m]	20.000	
Grid Width [m]	25.000	
Turbulence Model	IEC Kaimal spectral normal turbulence model	
No. of Vertical Grid-Points	51	
No. of Horizontal Grid-Points	63	
Turbulence Intensity [%]	13.715	12.087
Reference Wind Speed [m/s]	13.970	7.325
Reference Height [m]	12.500	
Wind Profile Type	IEC, Power law on rotor disk, logarithmic elsewhere	
Power Law Exponent	0.140	
Surface Roughness Length [m]	0.030	

Verification of Wave Conditions

In the initial FAST simulation runs, the irregular waves were simulated in FAST by assuming that the energy distribution follows the PM spectrum (the JONSWAP spectrum was not used because of the less pronounced peak shown in Fig 7). The wave parameters used in the FAST simulation were obtained from the 1-hr averaged data observed by the AWAC; however, the wave spectrum was not represented well, particularly in the lower frequency region. The wave and current data available from the AWAC were averaged to 1-hour readings, so there will be inaccuracy in the simulation results as wave and current properties may differ significantly within the 1-hour sampling period. Also the wave conditions at the system location may be bimodal/multimodal in nature, which cannot be represented from the 1-hr averaged data from the AWAC, because it only returns the peak frequency and period.

Therefore, a user-defined wave spectrum was entered into FAST from the wave spectrum obtained from the 10-min wave height data from the tower wave height sensor. The mean wave direction was obtained from the 1-hr averaged data observed by the AWAC. This process was performed for both cases and the time- and frequency-domain comparisons of the waves generated in FAST and the experimental data is shown in Fig. 7 and Fig 8. The wave spectrums in these figures do not match perfectly due to processing only the latter 10 minutes of the waves generated from 20 minutes in FAST. The time histories are also

not expected to match because phases of the simulated wave time history are random.

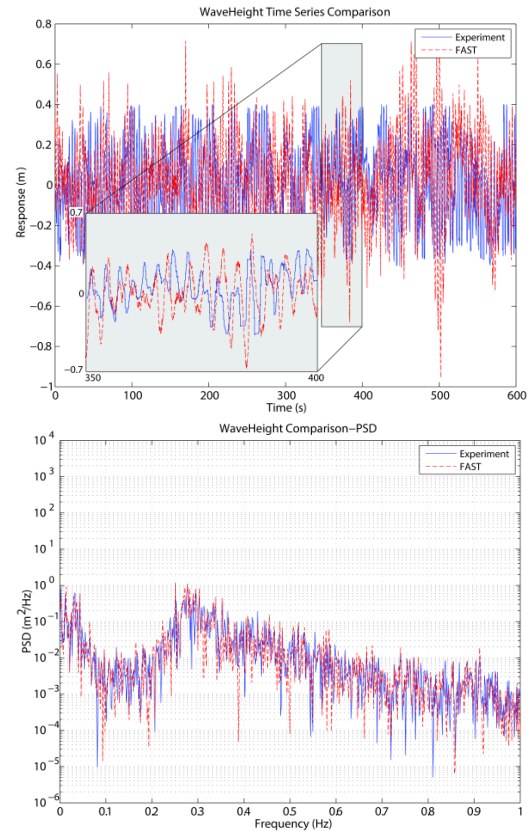


Fig. 7. Wave elevation comparison for the Non-Op Case.

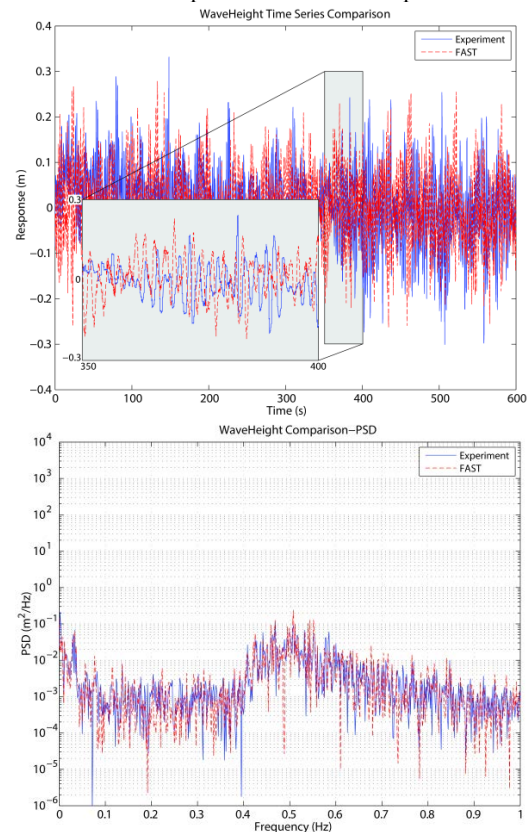


Fig. 8. Wave elevation height comparison for the Op Case.

Simulation Issues and Assumptions

During the model building stage, the transition point from the tower to the platform was set at the MSL. The simulations were conducted assuming that the MSL remained constant, but tidal changes caused this value to shift at different periods in time. It was not possible to directly represent this tidal variation within FAST without making many changes to the input files, so the tidal variation was therefore ignored in the analysis. The tide level could have a strong influence on the system behavior because it will change the displacement of the structure and therefore the stiffness in the mooring line, which will in turn affect the pitch/roll motion of the structure.

Because of the asymmetric stiffening of the tower by the spreader beam system that cannot be modeled by FAST, the tower was simplified to represent a rigid structure. This might cause an under-prediction of the pitch/roll motion of the system caused by localized bending of the tower.

After the de-commissioning of the turbine in December 2013, some water was detected in one of the built-in ballast tanks positioned just below the MSL (assumed to be emptied in the FAST model). As a result, the water in the ballast tank may have raised the center of gravity higher than what has been assumed, which in turn causes an increase of the pitch and roll periods.

The mean wave and current direction data provided from the AWAC were averaged to 1-hour readings, which may cause inaccuracy in the simulation results because wave and current properties may differ significantly within the 1-hour sampling period. Also, the AWAC was located about 12.5 m away from the wind turbine system in areas close to rock and contour regions. These circumstances reduced the confidence in the wave and current data obtained. The FAST simulation was therefore conducted with no current conditions.

From the wave verification results mentioned earlier, we also observed that the wave spectrum at the SWAY location may be bi-modal and multidirectional, which is likely a result of the close proximity of the system to the shore. From both the AWAC and the tower wave height sensor, it was not possible to accurately define the peak period, significant wave height and wave directions for all the different wave modes. Even if the full wave definitions were available, FAST v7 does not allow users to represent multidirectional waves.

For the Non-Op Case, the blades were pitched at 90 degrees (out of the wind). It is assumed for the FAST simulations that the turbine is operating at a constant rotor speed and blade pitch angle for both cases. The simulations were set at constant values because access to the control algorithms for the blade pitch and generator speed used on the SWAY turbine were not available. The lack of control will result in significant differences between the simulation and experiment.

Results

Tables 3 and 4 show the mean and standard deviation values for the pitch, surge, roll and sway motion of the wind turbine over the 10-min period for the Non-Op and Op Case, respectively. The corresponding power spectral density (PSD) plots are shown in Fig. 9 and Fig 10.

Table 3. Mean and standard deviation for DOFs for the Non-Op Case.

DOFs	Experiment	FAST (with Tower Load)	FAST (w/o Tower Load)
Pitch (Mean)	10.73092 °	7.35102 °	5.13869 °
Pitch (Std)	2.02462 °	2.20998 °	1.87538 °
Surge (Mean)	2.84368 m	2.18756 m	1.52206 m
Surge (Std)	0.52778 m	0.61528 m	0.52537 m
Roll (Mean)	-1.86967 °	-0.12633 °	-0.10568 °
Roll (Std)	2.04729 °	0.65069 °	0.63543 °
Sway (Mean)	1.02630 m	0.04125 m	0.03307 m
Sway (Std)	0.56352 m	0.18503 m	0.17650 m

Table 4. Mean and standard deviation for DOFs for the Op Case.

DOFs	Experiment	FAST (with Tower Load)	FAST (w/o Tower Load)
Pitch (Mean)	12.90595 °	13.95103 °	12.69992 °
Pitch (Std)	1.05561 °	2.63459 °	2.54336 °
Surge (Mean)	6.76051 m	4.03822 m	3.69268 m
Surge (Std)	0.34020 m	0.72369 m	0.71435 m
Roll (Mean)	1.63395 °	-1.43630 °	-1.30943 °
Roll (Std)	0.66471 °	0.98300 °	1.03791 °
Sway (Mean)	0.31973 m	-0.32309 m	-0.29564 m
Sway (Std)	0.19840 m	0.18473 m	0.19001 m

Discussion

Tower loading vs. no tower loading

For the Non-Op Case, one can observe from Table 3 that the mean pitch increased from 5.14° without tower loading to 7.35° with tower loading whereas the mean surge also increased from 1.52 m to 2.19 m. The standard deviations of pitch and surge also increased from 1.88° to 2.21° and 0.53 m to 0.62 m respectively. These data show that wind loading does have a significant effect on the dynamics of the SWAY turbine. Similarly for the Op Case in Table 4, the mean pitch increased from 12.70° to 13.95°, whereas the mean surge increased from 3.69 m to 4.04 m upon introducing wind loading to the tower. This increase is less significant than in the Non-Op Case because the dominant loading of the wind turbine system occurs on the wind turbine blades.

The wind is more dominant in the surge/pitch direction of the system and there are minor crosswind effects on the system. The minor crosswind effects are reflected in the small increases in the mean and standard deviation values of the roll and sway values shown in Tables 3 and 4.

From Fig. 9 and Fig 10, one can observe that the inclusion of the wind loading on the tower does not affect the PSD plots significantly. Only minor increases throughout the entire range of frequency for all DOFs are seen, because the wind inflow generated from TurbSim is random and generally decays with increasing frequency.

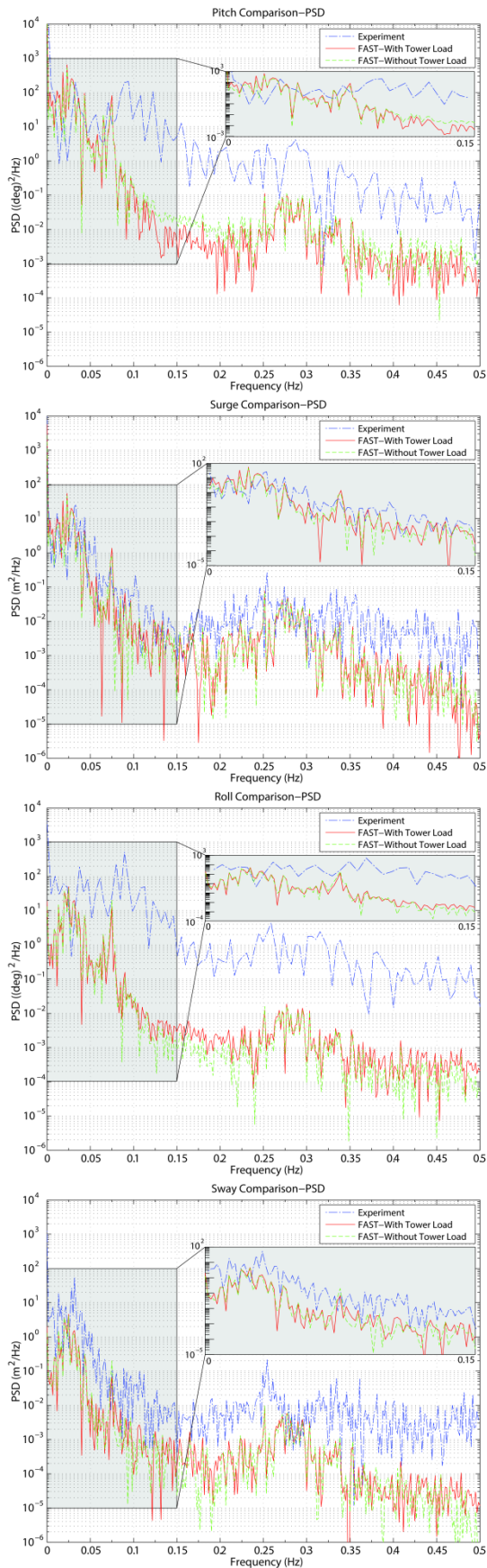


Fig. 9. PSD plots for DOFs for the Non-Op Case.

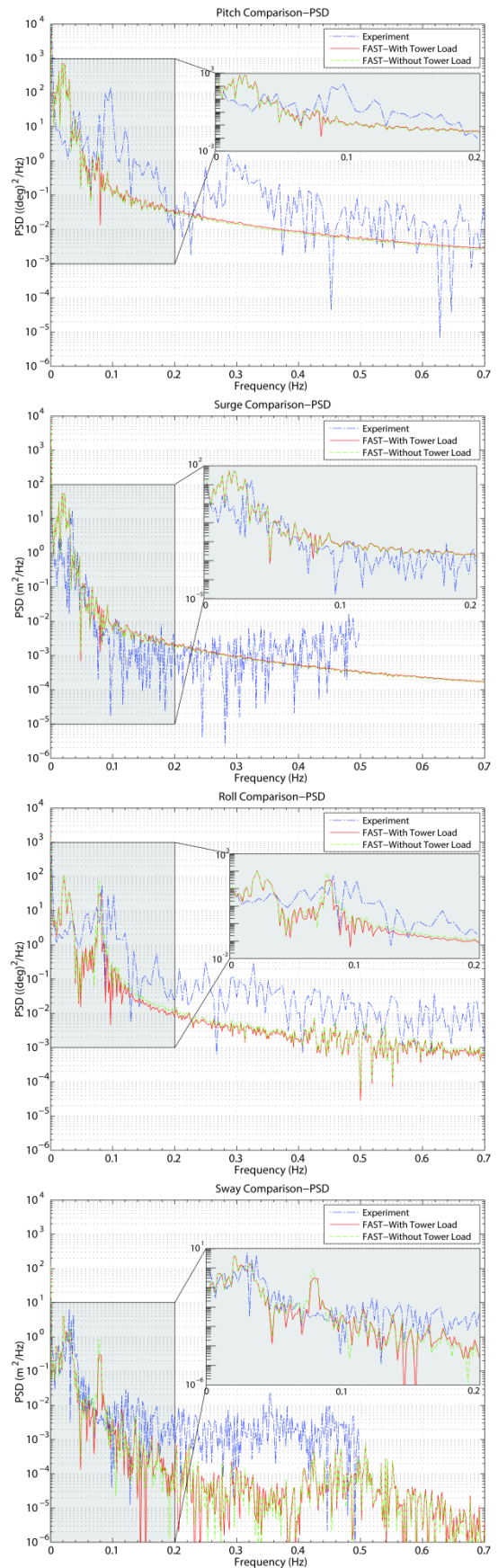


Fig. 10. PSD plots for DOFs for the Op Case.

Experiment vs. simulation

When comparing the simulated data with experimental data, Table 3 shows that simulating the wind loading on the tower increased the accuracy of the results for the surge and pitch component for the Non-Op Case. The improvement of accuracy is less evident in the Op Case in Table 4. This result is expected because the thrust loads on the rotor dominate the loading of the system in the operating condition. Also for the Op Case, the standard deviations for pitch and surge are less for the experiment compared to the simulation. This difference probably occurs because the control system in the experiment is reducing the variations of the thrust loads on the rotor, which again reduces the tower motions.

For both cases, Tables 3 and 4 show that the roll and sway simulation data are significantly deviating from the experimental observations. The roll and sway motions of the system are more influenced by the waves and current experienced by the system. As discussed earlier, no current conditions were set for the simulation and wave directions for the different wave modes were not well understood. Therefore, the errors and incoherence of the experimental data with simulation data is obvious in the roll and sway DOFs.

In the frequency domain for the Non-Op Case, the simulated data show significant frequency peaks at 0.025 Hz, 0.07 Hz and 0.28 Hz (Fig. 9). The 0.025-Hz and 0.28-Hz frequency peaks result from wave excitation, as is evident from the wave spectrum in Fig. 7 which shows corresponding peaks. The 0.07-Hz frequency peak is caused by the natural frequency of the entire system in the roll and pitch DOFs, which is discussed further in the earlier work of Koh et al. (2013). For the experimental data, the peaks at 0.025 Hz and 0.28 Hz are less defined but are observable in the PSD plots. The pitch/roll natural frequency of the system has shifted to 0.1 Hz and this is likely caused by a change in tidal conditions, compared to what is modeled.

The difference in magnitude between simulation and experiment for the PSD plots in the Non-Op Case is quite significant. In particular, the pitch and roll PSD plots for the experiment are much higher than the simulated results. This difference is likely caused by the lack of more detailed wind data and the inability to model the wave and current conditions accurately. The other simulation issues and assumptions as discussed earlier would also bring about more of the errors that are observed in the plots.

For the Op Case, the magnitude of the PSD plots compare well between the simulation and experiment. The simulated data for all DOFs show a significant frequency peak at around 0.022 Hz, which corresponds to the wave spectrum in Fig. 8 with a peak at 0.033 Hz. For the experimental data, the wave influence is represented by a peak occurring at about 0.35 Hz for all DOFs. Another peak is more evident for the simulated roll and sway DOFs, and is observed at around 0.08 Hz. This peak is also represented in the experiment data for roll and pitch DOFs at about 0.085 Hz. This frequency peak was caused by the natural frequency of the system. The wave frequency peak at about 0.5 Hz in Fig. 8 influenced the experimental sway and surge DOFs plots, but the observation is limited by the range of frequencies because of the sampling rate of the sensor.

CONCLUSION

In this study, a FAST model of the spar-type 1:6.5 scale prototype SWAY system was built with the design descriptions made available by SWAY AS. Different modeling strategies and assumptions were used to enable the model to work without major changes to the FAST tool.

During the initial runs of the simulation cases, it was noted that wind loading on the tower may be important in the analysis of floating turbines—particularly for the SWAY prototype that has a large tower relative to the size of the rotor—and in conditions in which the turbine blades are not operating.

Changes were made to the FAST code to account for the wind loading on each tower element for each simulation time step. Although the improvements are focused on tubular tower designs, code users have the option to manually enter the drag coefficient of the tower or to utilize the provided $Re-C_{D,tower}$ table applicable for a circular smooth tower.

One nonoperating test case with a significant wave height of 0.65 m and mean wind speeds of 13.97 m/s, and one operating test case with turbine rotating at mean rotational speed 33.67 rpm with mean wind speed of 7.32 m/s were selected from the available data for a validation study.

The results show that wind loading on the tower does have a significant effect on the response of the wind turbine system when it is not operating (in high wind speeds). The wind loading on the tower has a less significant effect when the system is operating because the dominant loading on the wind turbine system occurs on the wind turbine blades. Including the wind loading on the tower increased the accuracy of the simulation results in comparison with the experimental results for the nonoperating conditions.

The key reasons for the errors between the results of the simulation and experiment follow. First, the FAST model is unable to model the wave conditions accurately, due to the limited wave data available and limitations of FAST in representing the possible multidirectional nature of the waves. The near-shore location of the turbine creates very complicated wave forms because of the reflection of the waves from the shore. Second, tidal variations were excluded in the model due to the inability of FAST to simulate them easily without major changes to the input files. Third, current conditions were excluded because of the reduced confidence of the AWAC readings that resulted from its location and data-averaging frequency. Fourth, no control system was included for the operational case. Other uncertainties/assumptions in the modeling and issues with setting up the instrumentation on the prototype may have also contributed to the errors observed.

Although mixed results were observed in comparing the system behavior between the experiment and FAST simulations, this study was useful in building competencies, learning and understanding the key issues and challenges in an open-sea validation study, and identifying some limitations in the modeling approach. Unlike laboratory testing, the complex nature of the environment and the inability to fully characterize its influence on the system is one of the key challenges in validating a model using open-sea data. In addition, the lack of a control system significantly limited the ability to accurately represent the turbine behavior.

Future work may look at quantifying the assumptions and estimating the resulting errors. A simple control system may be considered, and the model fidelity may be increased to reduce assumptions. Some changes to the FAST tool might include altering the mooring-line model to better represent the tension-rod system, accounting for nacelle drag forces, addressing the ability to model different tide levels, and including the capability to model multidirectional waves. In fact, a newer version of FAST (v8.09.00a-bjj), made available in September 2014, includes the ability to model multidirectional waves, but this work was done prior to its release. The complexity of the present

location of the SWAY system, however, may preclude the ability to model the wave conditions accurately, even with multidirectional waves, because of the inability to accurately measure the conditions.

ACKNOWLEDGEMENTS

The authors gratefully acknowledge the support provided by the Energy Research Institute at Nanyang Technological University. In addition, the expertise and support of SWAY AS in conducting the model test and providing valuable test data is greatly appreciated. This work was supported by the U.S. Department of Energy under Contract No. DE-AC36-08GO28308 with the National Renewable Energy Laboratory. Funding for the work was provided by the DOE Office of Energy Efficiency and Renewable Energy, Wind and Water Power Technologies Office.

REFERENCES

- Bak, C., Madsen, H. A., Johansen, J. (2001). Influence from blade-tower interaction on fatigue loads and dynamics (poster). Paper presented at the European Wind Energy Conference and Exhibition 2001, Copenhagen, Denmark.
- Bir, G. S. (2007). User's Guide to BModes (Software for Computing Rotating Beam Coupled Modes).
- Du, Z., Selig, M.S. (1998). A 3-D stall-delay model for horizontal axis wind turbine performance prediction. Paper presented at the Proceedings of 36th AIAA Aerospace Sciences Meeting and Exhibit, Reno, NV.
- Eggers, A.J., Digumarthi, R.V. (1992, 1992). Approximate Scaling of Rotational Effects on Mean Aerodynamic Moments and Power Generated by CER Blades Operating in Deep-Stalled Flow. Paper presented at the 11th ASME Wind Energy Symposium, Houston, Texas.
- Engineering Sciences Data Unit. (1986). ESDU 80025 Mean forces, pressures and flow field velocities for circular cylindrical structures: single cylinder with two-dimensional flow.
- European Committee for Standardization. (2005). EN 1991-1-4:2005 Eurocode 1. Actions on structures. General actions. Wind actions.
- Holmes, J. D. (2007). Wind loading of structures: London ; New York : Taylor and Francis, 2007. 2nd ed.
- International Electrotechnical Commission. (2009). IEC 61400-3 Design requirements for offshore wind turbines.
- International Organization for Standardization. (2009). ISO 4354:2009 Wind actions on structures (pp. 68).
- Jonkman, B.J., Jonkman, J.M. (2013). Addendum to the User's Guides for FAST, A2AD, and AeroDyn.
- Jonkman, B.J., Kilcher, L. (2012). TurbSim User's Guide: Version 1.06.00. Golden, CO.
- Jonkman, J. (2014). FAST Theory Manual. Golden, CO: National Renewable Energy Laboratory (forthcoming)
- Jonkman, J., Buhl, M.L.J. (2005). FAST User's Guide.
- Jonkman, J.M. (2007). Dynamics Modeling and Loads Analysis of an Offshore Floating Wind Turbine. (Ph.D. dissertation), University of Colorado, United States.
- Jonkman, J.M. (2009). Dynamics of offshore floating wind turbines—model development and verification. *Wind Energy*(June), 459-492. doi: 10.1002/we
- Koh, J.H., Robertson, A.N., Jonkman, J.M., Driscoll, F., Ng, E.Y.K. (2013). Building and Calibration of a FAST Model of the SWAY Prototype Floating Wind Turbine. Paper presented at the International Conference on Renewable Energy Research and Applications (ICRERA) 2013, Madrid, Spain.
- Laino, D., Hansen, A. C. (2002). Aerodyn User's Guide.
- Moriarty, P.J., Hansen, A.C. (2005). AeroDyn Theory Manual.
- Powles, S.R.J. (1983). The effects of tower shadow on the dynamics of a horizontal-axis wind turbine. *Wind Engineering*, 7, 26-42.
- Roshko, A. (1961). Experiments on the flow past a circular cylinder at very high Reynolds number. *Journal of Fluid Mechanics*, 10(03), 345-356. doi:10.1017/S0022112061000950
- Scruton, C. (1981). An introduction to wind effects on structures: London : Oxford University Press for the Design Council, the British Standards Institution and the Council of Engineering Institution, c1981.
- Scruton, C., Rogers, E.W.E., Menzies, J.B., Scorer, R.S. (1971). Steady and Unsteady Wind Loading of Buildings and Structures [and Discussion] (Vol. 269).
- Viterna, L.A., Janetzke, D.C. (1982). Theoretical and experimental power from large horizontal-axis wind turbines. United States, : National Aeronautics and Space Administration.
- WAMIT, I. (2012). WAMIT User Manual Version 6.4: Dept. of Ocean Engineering, Massachusetts Institute of Technology.
- Wieselsberger, C. (1921). Neuere Feststellungen über die Gesetze des Flüssigkeits- und Luftwiderstandes. *Phys. Z*, 22, 321–328.